This article has been accepted for publication in a future issue of this journal, but has not been fully edited. Content may change prior to final publication. Citation information: DOI 10.1109/TAES.2019.2961826, IEEE Transactions on Aerospace and Electronic Systems

Star identification based on spider web image and hierarchical CNN

First A. Author, *Fellow, IEEE*, Second B. Author, and Third C. Author, Jr., *Member, IEEE*

***Abstract*—Unlike traditional star pattern recognition algorithms that extract star features as a vector to be matched in a database, a spider web image is constructed and a hierarchical convolution neural network model is proposed to recognize this spider web image. Stars are linked with different color lines based on angle distance to enhance discrimination of spider web images. A training dataset and testing dataset are constructed based on spider web images for Convolution neural networks (CNN) model training. A hierarchical CNN model with two stages, which are designed to perform first step identification and recognize similar spider web images, respectively, is proposed. Experiment results show that, compared with other algorithms, the proposed algorithm is more robust toward position noise, magnitude noise, small numbers of stars in the field of view (FOV), and the presence of false stars.**

***Index Terms*—Enter key words or phrases in alphabetical order, separated by commas. For a list of suggested keywords, send a blank e-mail to keywords@ieee.org or visit http://www.ieee.org/organizations/pubs/ani_prod/keywrd98.txt**

I. Introduction

STAR trackers, precise devices used to determine spacecraft attitude, are the most extensively adopted celestial navigation instrument [1-3]. Star trackers mainly operate through three procedures: star centroid extraction, star identification, and attitude calculation. Of these procedures, the star identification algorithm is the foundation for calculating spacecraft attitude.

The first star identification algorithm was proposed by Junkins in 1970 [1 – 3], and after this, many other star identification algorithms, such as image correlation matching [4], singular value decomposition [5], and optimal image matching [6,7] have been proposed. Meng Na and Benjamin surveyed star identification algorithms developed in recent years [8, 9]. Star identification algorithms consist of two classes: subgraph isomorphism and pattern recognition algorithms. Subgraph algorithms include the triangle algorithm [10, 11], pyramid algorithm [12, 13], geometric voting algorithms, [14] and match group algorithm [15]. The triangle algorithm, which is one of the most popular star identification algorithms, has been extensively studied and widely used [11], and has good robustness toward false and missing stars in the field of view (FOV). However, the triangle algorithm is susceptible to star position noise and it typically has high memory requirements and calculation time [10].

Pattern recognition algorithms, another star identification algorithm class, take the geometric distribution of a main star and its neighboring stars as star pattern, which the algorithm then uses to distinguish the main star from other stars [8, 9]. The grid algorithm, a classical star identification algorithm proposed by Padgettin in 1997 [16], performs well in the presence of position noise and requires fewer computer resources. Subsequently, some modified grid algorithms were proposed by Daniel S. Clouse and Meng Na [17, 18]. Nevertheless, grid algorithms are susceptible to magnitude noise, missing stars, and false stars in the FOV. The polestar algorithm, proposed by Bittanti in 2006 [19], surmounts the grid algorithm's shortcomings; however, this algorithm is not comparatively stable toward false stars in the FOV [20, 21]. The radial and neighboring distributions of stars are harnessed in a unified redundant pattern proposed by Jiang [22], which improves algorithm accuracy when there are only a few stars in the FOV and has short calculation time. However, this method is not robust toward position noise and magnitude noise.

Convolution neural networks (CNN) have achieved great image classification, such as star identification, and object detection results in recent years [23]. Unlike conventional pattern recognition algorithms that extract star features as a vector to be matched in a database, the method in this study transforms information on a main star and its neighboring stars into a spider web image with different color lines that can enhance discrimination of different stars, and Additionally a hierarchical CNN model is proposed to recognize this spider web image. A training dataset and testing dataset were also constructed.

The remainder of this paper is organized as follows. Section II describes the construction of the spider web image, training data, and test data, and shows the proposed model's architecture. Section III discusses experiment results for

This paragraph of the first footnote will contain the date on which you submitted your paper for review. It will also contain support information, including sponsor and financial support acknowledgment. For example, "This work was supported in part by the U.S. Department of Commerce under Grant BS123456."

The next few paragraphs should contain the authors' current affiliations, including current address and e-mail. For example, F. A. Author is with the National Institute of Standards and Technology, Boulder, CO 80305 USA (e-mail: author@ boulder.nist.gov).

S. B. Author, Jr., was with Rice University, Houston, TX 77005 USA. He is now with the Department of Physics, Colorado State University, Fort Collins, CO 80523 USA (e-mail: author@lamar.colostate.edu).

T. C. Author is with the Electrical Engineering Department, University of Colorado, Boulder, CO 80309 USA, on leave from the National Research Institute for Metals, Tsukuba, Japan (e-mail: author@nrim.go.jp).

This article has been accepted for publication in a future issue of this journal, but has not been fully edited. Content may change prior to final publication. Citation information: DOI 10.1109/TAES.2019.2961826, IEEE Transactions on Aerospace and Electronic Systems

synthesized and real star images and their comparison. Finally, a conclusion is provided in Section IV.

II. Guidelines For Manuscript Preparation

The proposed algorithm can be divided into four parts as indicated in Fig. 1. First, the spider web image's construction rule is defined. Second, training and testing datasets are constructed based on the rule in step 1. Third, a hierarchical CNN model for recognizing spider web images is proposed and trained with the datasets produced in step 2. Lastly, a real star image is transformed into a spider web image based on the rule in step 1 and the proposed hierarchical CNN model is adopted to recognize it.

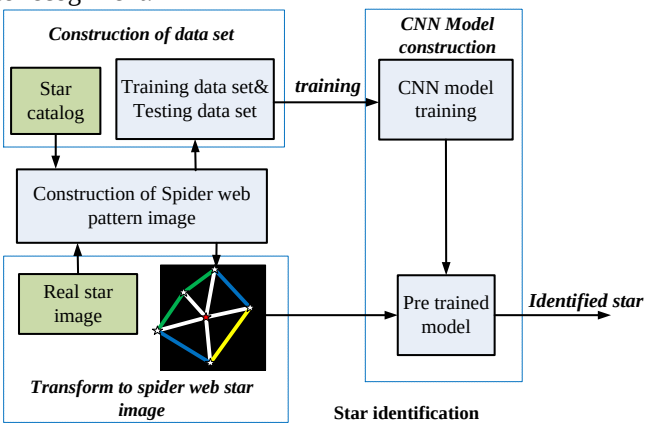

Fig.1. Flow chart of the proposed star identification algorithm

A. Abbreviations and Acronyms

Unlike conventional pattern recognition algorithms, which extract star features as a vector to be matched in a database, the algorithm in this paper transforms the main star and its neighboring stars into a spider web image that the CNN will recognize. This method is established as follows:

First, pattern radius R and the main star to be recognized are selected, and stars within the main star's pattern radius are considered neighbor stars as indicated in Fig. 2 (a), (b). Next, the main star and neighboring stars are linked with white lines (Fig. 2(c)) and the distances between adjacent neighboring stars are calculated. Supposing that stars A and B have coordinates of (X_1,Y_1) and (X_2,Y_2) and focal length is f, the angular distance under the star sensor coordinate system can then be defined as

$$d_m^{12} = \cos^{-1}\left(\frac{s_1 \cdot s_2}{|s_1| \cdot |s_2|}\right) \tag{1}$$

$$s_1 = \frac{1}{\sqrt{X_1^2 + Y_1^2 + f^2}} \begin{pmatrix} X_1 \\ Y_1 \\ -f \end{pmatrix} \qquad s_2 = \frac{1}{\sqrt{X_2^2 + Y_2^2 + f^2}} \begin{pmatrix} X_2 \\ Y_2 \\ -f \end{pmatrix} \tag{2}$$

Here, s_1 and s_2 are direction vectors under the star sensor coordinate system. Finally, to enhance the discrimination of different spider web images and increase information on the spider web image, adjacent neighboring stars are linked by different color lines based on angle distance between them (Fig. 2 (d)). Table 1 details the relationship between angle distance and line color. In Fig. 2 (b), the red star represents main star, whereas the white stars represent neighboring stars.

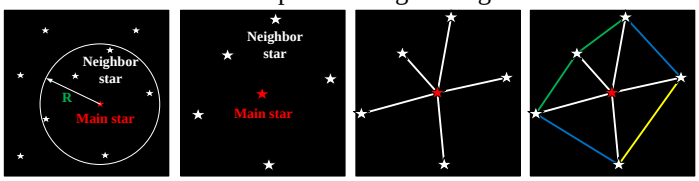

Fig.2. Construction of spider web images. (a) Selection of main star and pattern radius. (b) Main star and its neighboring stars. (c) Linking of main star and its neighboring stars. (d) Linking of neighboring stars

Table 1 Relationship between angle distance and line color

Angle distance/ °0~2	2~4	4~6	6~8	8~10	10~12
Color	red	green	blue	yellow	cyan	purple

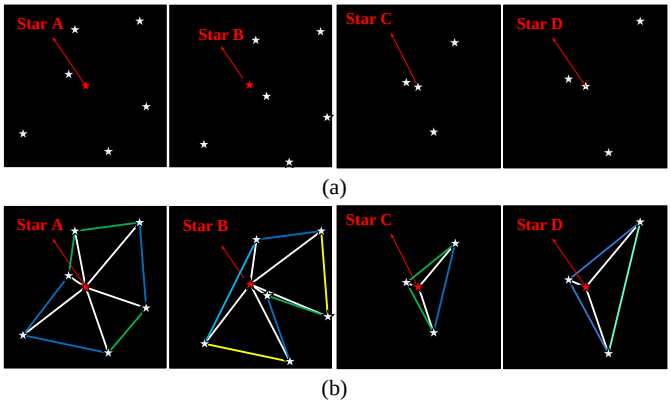

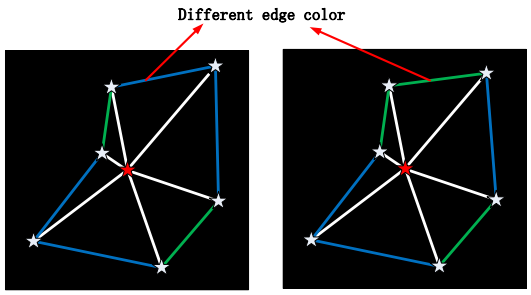

Fig.3. (a) Star image without line segments. (b) Spider web image with line segments. (c) Different line colors caused by position noise.

For two main stars that are comparatively close to each other, such as stars A and B in Fig. 3, the two-star images are more like a shift transformation without line segments. After different color line segments are added, the spider web images of two main stars are easily distinguishable. When two main stars have similar neighboring star distributions, such as stars C and D in Fig. 3, the star image of C resembles a scale transformation of D's star image. However, once adjacent neighboring stars are linked with different color lines based on

This article has been accepted for publication in a future issue of this journal, but has not been fully edited. Content may change prior to final publication. Citation information: DOI 10.1109/TAES.2019.2961826, IEEE Transactions on Aerospace and Electronic Systems

angle distance, the spider web images of two main stars are easily distinguishable.

B. Other Recommendations

To train the hierarchical CNN model in the next step, training and testing datasets are constructed based on star pattern criteria.

Stars with magnitudes less than 6 were selected from the Smithsonian Astrophysical Observatory catalog to construct spider web image training data. The pattern radius is 6 °except in cases where there are fewer than four stars in the FOV. Thus, 4051 stars are selected. To ensure that each star's training set contains different angles, star images were rotated 30 °until it covered 360 °. Thus, 12 star images with different angles are included in the dataset. To enhance the algorithm's robustness to false stars, one or two false stars were added randomly 10 times to star images of each angle; therefore, each star has 130 training samples. The spider web images were then constructed based on step 1, producing a training set of 486,120 training samples with 4051 classes. Figure 4 shows a sample of the training set.

The relative positions of stars is fixed, thus the primary differences between spider web images are rotation and false stars. To verify the algorithm's robustness toward different angles, the test set uses a different rotation angle than the training set. The spider web image was rotated every 70 °, thus, six star images with different angles were included until it covers 360 °. We randomly added one or two false stars five times to star images of each angle. One star thus has 30 test spider web images and the test set has 121,530 samples. Figure 4 shows samples of training and testing dataset images.

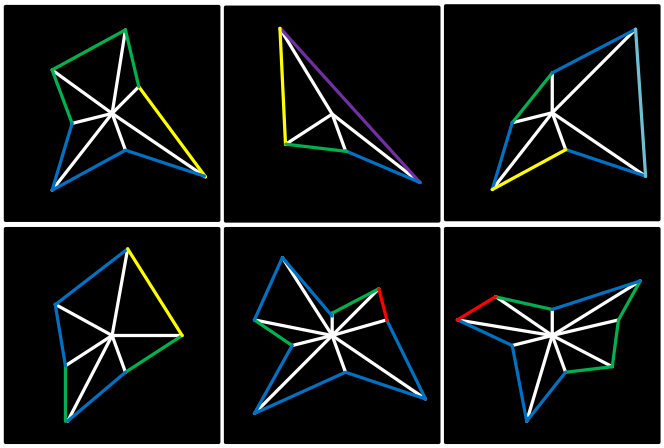

Fig. 4. Sample spider web images from training and testing datasets

C. CNN model

I. Convolutional neural network

First proposed by Y. LeCun [24], a CNN is a critical type of feed-forward neural network with multilevel learnable representations. It achieved better results in image classification [25], segmentation [26], and object detection [27] than conventional methods. The typical architecture of a CNN consists of convolutional layers, pooling layers, activation layers, and fully connected layers. Compared with a traditional neural network, a CNN decreases the number of weights and simplifies network model complexity to a great extent. More importantly, a CNN has good robustness toward image rotation, translation and small deformation. In light of these features, a CNN model is proposed in this paper to classify spider web images.

II. Architecture of CNN model

Considering that the training dataset contains more than 4000 classes of spider web star image a, some with similar shapes, it is very difficult for a simple CNN model to achieve high accuracy. To tackle this problem, we proposed a two-stage hierarchical CNN model.

2.1 Overview of the proposed hierarchical CNN model

As shown in Fig. 5, the proposed model consists of two stages that have the same elementary feature in the first layer as similar spider web images have similar low-level features, such as edges and anchors. In the first stage, spider web images are classified into M classes, which results in high prediction probability for direct star identification and low prediction probability for similar spider web images (Fig. 6), thus further classification is required. In the second stage, K special classifiers are designed to classify similar spider web images, with only spider web images with similar shapes used to train these classifiers. Similar spider web images belonging to different groups have different high-level features and can thus be distinguished in the second stage. Because only several similar spider web images are in each set, the second stage has remarkably reduced calculation time. In Fig. 5, N_k represents the number of similar spider web images in the K th similar spider web images set.

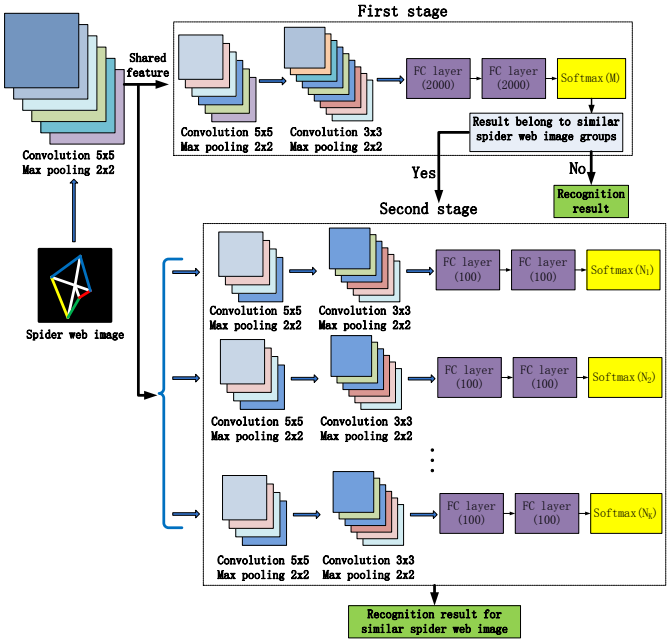

Fig.5. Architecture of spider web model

This article has been accepted for publication in a future issue of this journal, but has not been fully edited. Content may change prior to final publication. Citation information: DOI 10.1109/TAES.2019.2961826, IEEE Transactions on Aerospace and Electronic Systems

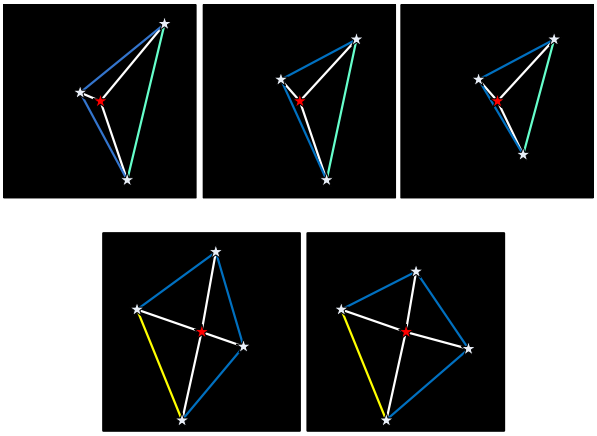

Fig.6. Several similar spider web images

2.2 Definition of similar spider web images

The definition of similar spider web images is based on the hierarchical CNN model's first stage classification results. This only achieves a 90.2% accuracy for all spider web images as some similar spider web images exist in the dataset. The prediction probabilities of these images are relatively low, which reduces accuracy. Therefore, we extracted similar spider web images to perform further classification in the second stage. The outputs of the softmax classifier can be defined as

$$h_\theta(x^{(i)}) = \begin{bmatrix} p(y^{(i)}=1 \mid x^{(i)};\theta) \\ p(y^{(i)}=2 \mid x^{(i)};\theta) \\ \vdots \\ p(y^{(i)}=3 \mid x^{(i)};\theta) \end{bmatrix} = \frac{1}{\sum_{j=1}^{k} e^{\theta_j^T x^{(i)}}} \begin{bmatrix} e^{\theta_1^T x^{(i)}} \\ e^{\theta_2^T x^{(i)}} \\ \vdots \\ e^{\theta_k^T x^{(i)}} \end{bmatrix} = \begin{bmatrix} p_{i1} \\ p_{i2} \\ \vdots \\ p_{ik} \end{bmatrix} \quad (3)$$

$$p_{ij} = \frac{e^{\theta_j^T x^{(i)}}}{\sum_{j=1}^{k} e^{\theta_j^T x^{(i)}}} \quad (4)$$

where $x^{(i)}$ denotes the activation vector of ith sample at the previous layer in the softmax classifier and θ_j^T is the weight vector connected to the jth neuron in the softmax layer. $p(y^{(i)} = j \mid x^{(i)};\theta)$ indicates the probability of the ith sample belonging to the jth category. Thus, the softmax classifier's output is the probability of $x^{(i)}$ of each category. The similarity of spider web images i and j is defined as S_{ij}, which can be expressed as

$$S_{ij} = \frac{1}{Q}\sum_{q=1}^{Q} p_{ij}^q + \frac{1}{Q'}\sum_{q=1}^{Q'} p_{ji}^q = \frac{1}{Q}\sum_{q=1}^{Q} \frac{e^{\theta_i^T x^{(i)}}}{\sum_{j=1}^{k} e^{\theta_j^T x^{(i)}}} + \frac{1}{Q'}\sum_{q=1}^{Q'} \frac{e^{\theta_i^T x^{(j)}}}{\sum_{j=1}^{k} e^{\theta_i^T x^{(j)}}} \quad (5)$$

where p_{ij}^q corresponds to the probability that the qth training data of ith spider web image is classified to the jth spider web image, whereas Q is the number of these images in training dataset. We extract S_{ij} values greater than S_T (a pre-defined threshold obtained from experiment results) and corresponding spider web images are clustered into the same class. Thus, 227 classes including 494 spider web images are extracted. If the first stage classifies an input spider web image to one of these groups, the second stage performs further classification.

2.3 Parameters of the proposed CNN model

In the first stage, the structure of the model consists of eight layers. The first and second convolutional layers have 20 and 50 5 ×5 square filters, respectively, and the third convolutional layer has 200 3 × 3 square filters. Note that classical models such as Alex-Net, VGG-Net, and Google-Net [30] that take on numerous convolutional kernels are more compatible with images complex nature scenes, and thus are not suitable for spider web images with less information. To avoid overfit, we added filters in each convolution layer of the proposed model, and each convolutional layer is followed by max-pooling. Batch normalization is performed after the second and third convolutional layers, and a leaky ReLU is selected for non-linearity activation of each convolutional layer. The last two layers are fully connected layers, each with have 2000 filters. A dropout is added in the first fully connected layer to reduce over fitting and the last layer performs softmax classification. The training dataset and testing dataset were adopted to train the model. The structure in the second stage is similar to that in the first stage and we set the 100 neurons in fully connected layers for each classifier.

III. EXPERIMENT

Spider web images were formed based on spider web star pattern criteria. Experiments were carried out on a 4.0GHz desktop computer with a GTX1070 GPU, and programs were implemented in CAFFE. The average execution time per image was 2.2 ms.

A. Training the proposed model

The first stage CNN of the proposed model is critical to the second stage's performance. The first stage was trained on 4051 classes using the training dataset. Similar spider web image pairs were extracted based on first stage results. These star pairs were then selected to train the proposed model's second stage. Classifiers in the second stage were all trained separately using their corresponding training data. To train our CNN model, the gradients of the first stage CNN were back-propagated from the fully connected layer to the first layers, whereas the second stage CNN gradients did not change the weights in first layers and were only back-propagated to their own layers.

A. Experiment result

The proposed method belongs to the pattern recognition algorithms category, thus, classical star identification algorithms for pattern recognition were selected to compare the proposed algorithm's capabilities using synthesized and real star images. These algorithms include the grid [19], polestar [24], and unified redundant pattern algorithms [25]. The FOV of all algorithms was 20 ° × 20 °. Real star images were downloaded from ZY-3, a Chinese civilian satellite. Table 2 shows the synthesized star tracker's parameters. Position noise, magnitude noise, false stars, and missing stars were tested using the synthesized star images. The training and testing image sets differ from the experimental set. We selected different numbers of star images based on different types of noise in the experiment. For the training and testing images, we rotated the

This article has been accepted for publication in a future issue of this journal, but has not been fully edited. Content may change prior to final publication. Citation information: DOI 10.1109/TAES.2019.2961826, IEEE Transactions on Aerospace and Electronic Systems

images at different angles for data augmentation; however, we only selected one angle to create a spider web image for the experimental images.

Table 2 Synthesized star tracker parameters

Image plane dimension	2048 pixels × 2048 pixels
Pixel size	0.055 mm × 0.055 mm
FOV	20 ° × 20 °
Instrumental threshold	6.0 Mv

We added different standard deviations of position noise to the star centroid locations 10 times for each image to simulate the star location error because we tested eight different standard deviation position noises. We selected 16,000 images for the position noise experiment. Figure 7 illustrates the effects of position noise on the identification rates of different algorithms.

The CNN model is robust toward small deformations due to position noise. Thus, although the line colors of star pairs may change, the spider web image shape remains similar, which can help the CNN model recognize it. Unlike the other algorithms tested, the proposed algorithm is more robust toward position noise and achieves a higher identification rate. Compared with other algorithms, the purposed algorithm's identification rate subtly decreases as the standard deviations of position noise increase.

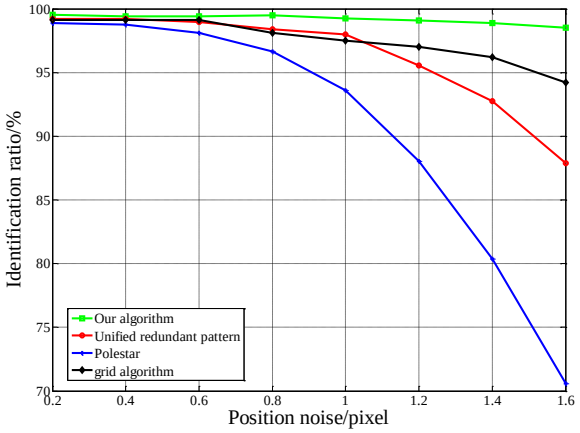

Fig.7. Effects of position noise on identification rate

We added different standard deviations of magnitude noise 10 times to each image to test the effects of star magnitude noise on the identification rate because we tested five different standard deviation magnitude noises. We selected 10,000 images for the magnitude noise experiment. Gaussian noises with standard deviations of σ_M = 0.3Mv to 0.98Mv were added to synthesized star images to simulate magnitude noise. As shown in Fig.8, the proposed algorithm's accuracy decreases as magnitude noise increases because magnitude noise causes missing and false stars. However, compared with other algorithms tested, the proposed algorithm has a higher identification rate with magnitude noise of different standard deviations.

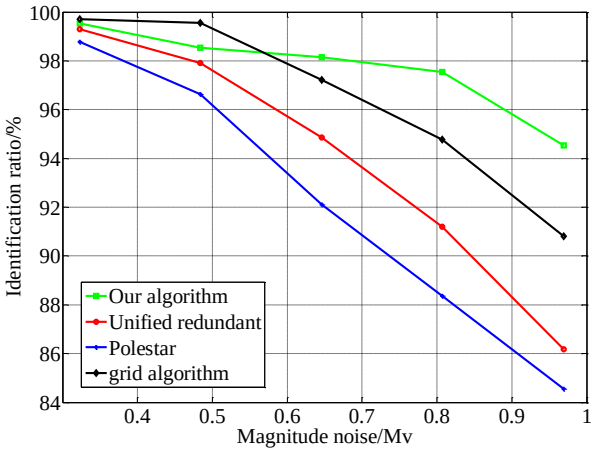

Fig.8. Effects of star magnitude noise on identification rate

Star images with more than four stars in the FOV were selected to ascertain the effects of the number of stars in the FOV on identification rates. At least four stars in the FOV are required by the star identification and attitude solution. Figure 9 shows that identification rates increase with the number of stars in the FOV. More stars in the FOV makes the spider web image more discriminative, thus increasing identification rates. When the number of stars is more than 10, no similarity in different spider web images occurs. Therefore, the proposed algorithm has a 100% identification rate in FOV with more than 10 stars. By contrast, conventional star identification algorithms can only achieve high identification rates when there are more than 15 stars in the FOV.

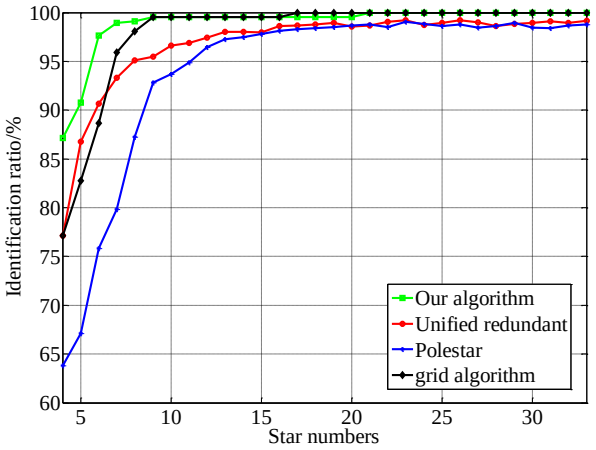

Fig.9. Effects of different star numbers on identification rates

Robustness toward false stars was also tested, and the results are presented in Fig. 10. We selected 12,000 images for false star experiment. The proposed algorithm achieves a higher accuracy than the unified redundant algorithm and polestar algorithm; however, the proposed algorithm's accuracy decreases with an increasing percentage of false stars.

This article has been accepted for publication in a future issue of this journal, but has not been fully edited. Content may change prior to final publication. Citation information: DOI 10.1109/TAES.2019.2961826, IEEE Transactions on Aerospace and Electronic Systems

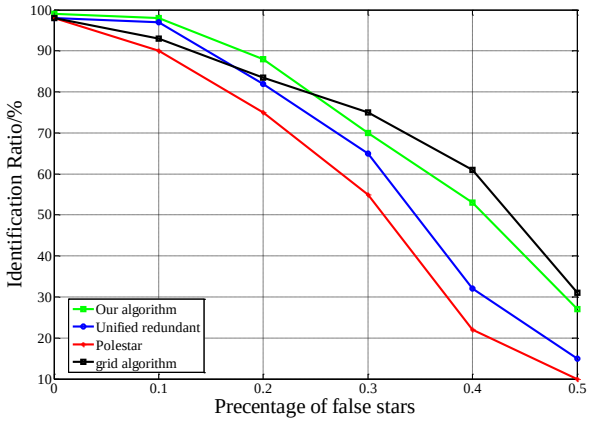

Fig.10. Effects of the percentage of false stars on identification rates

Because missing stars change the shape of a spider web image, it will significantly decrease the proposed algorithm's accuracy. We selected 10,000 star images to perform the missing star experiment and replaced varying numbers of stars with varying numbers of missing stars. The results are shown in Fig. 11, indicating that the proposed algorithm's accuracy will decrease as the number of missing stars increases.

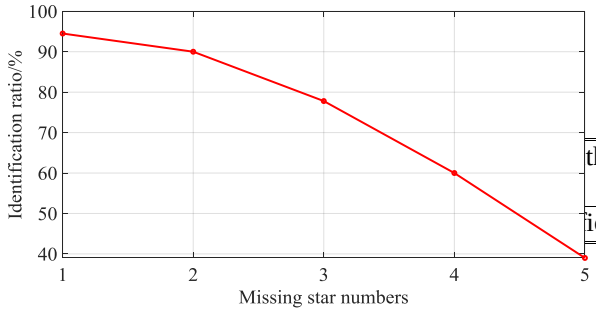

Fig.11 Effects of missing stars on identification rate

A total of 278 real star images were downloaded from ZY-3 to test the identification rate. Table 4 provides the parameters of the ZY-3 star tracker. Real star images ZY-3 and the main star to be recognized and pattern radius are shown in Fig. 12.

Table 4 Configurations of ZY-3 satellite star tracker

Image plane dimension	1024 pixels × 1024 pixels
Pixel size	0.015 mm × 0.015 mm
Focal length	43.258 mm
FOV	20 ° × 20 °

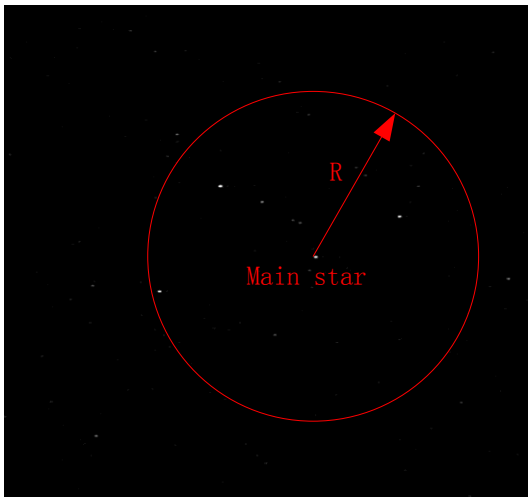

Fig.12 Real star image from ZY-3

Experimental results from the test of the three algorithms are given in Table 5. Five star images cannot be identified in our algorithm, in that most stars were near the edge of the star image. If the proposed criterion is used, then the range of the circle will be outside of the edge of the star image, and stars outside of the edge cannot be confirmed. Thus, the spider web image does not cover all the information of neighboring stars and cannot be recognized. Nevertheless, the proposed algorithm presents a comparatively higher identification rate than other star identification algorithms.

Table 5 Summary Result on Satellite Real Images

thm	Proposed algorithm	Polestar algorithm	Unified redunda algorithm
ication rate	98.16%	98.21%	94.64%

IV. Conclusion

This paper proposed using a spider web image to perform star identification through a hierarchical CNN model. Accordingly, different colored lines are used to link adjacent neighboring stars based on their angular distance, with the main star and its neighboring stars linked by white lines. These lines enhance the discrimination of different main stars, making it suitable for a CNN model to recognize. A hierarchical CNN model with two stages is proposed. Based on the first stage results, a method to automatically extract similar spider web images is provided. Similar spider web images are then classified in the second stage. The two stages share the same low-level features, which saved calculation time compared with deep network methods. Experiment results showed that, compared with other pattern recognition star identification algorithms, the proposed algorithm performs more robustly with respect to position noise, magnitude noise, and false stars, especially with higher noise standard deviations in synthesized star images. The proposed algorithm has a higher identification rate than other star identification algorithms with fewer star numbers in the FOV. Experiment results demonstrated that our algorithm achieved better identification rate than other

algorithms in simulated star images and performed better in cases with false stars. In real star images, our algorithm achieved an identification rate of 98.16%.

REFERENCE

[1] Liebe, C. C. "Star tracker for attitude determination." IEEE Transactions on Aerospace and Electronic Systems, 10, 6(1995), 10-16.DOI: 10.1109/62.387971

[2] Nicholas A. Truesdale, Michael A. Skeen, Jedediah Diller, Kevin Dinkel, Zach Dischner, Aaron Holt, Tyler Murphy, Sara Schuette and Andrew Zizzi. "DayStar: Modeling the daytime performance of a star tracker for high altitude balloons." 51th AIAA Aerospace Sciences Meeting including the New Horizons Forum and Aerospace Exposition, Grapevine, Texas, Jan. 2013.DOI: 10.2514/6.2013-139

[3] Junkins, J.L. and Strikwerda, T.E. "Autonomous star sensing and attitude estimation." Proc. Annual Rocky Mountain Guidence and control Conference, 1979.DOI: 10.1109/ISSCAA.2006.1627471

[4] Juang, J. N., Kim, H. Y. and Junkins, J. L. "An efficient and robust singular value method for star pattern recognition and attitude determination." Journal of Astronautical Science, 52, 1(2004), 211-220.

[5] Xinguo Wei, Guangjun Zhang and Jiejiang. "Star identification algorithm based on log-polar transform." Journal of Aerospace Computing, Information, and Communication, 6(2009), 483-490.DOI: /10.2514/1.30393

[6] Hyosang Yoon, Yeerang Lim and Hyochoong Bang. "New star-pattern identification using a correlation approach for spacecraft attitude determination." Journal of Spacecraft and Rockets, 48, 1(2011), 182-186.DOI: 10.2514/1.49675

[7] TjorvenDelabie. "A highly efficient attitude estimation algorithm for star trackers based on optimal image matching." AIAA Guidance, Navigation, and Control Conference, Minneapolis, Minnesota, Aug, 2012.DOI: 10.2514/1.61082

[8] Mengna and PeifaJia. "A survey of all-sky autonomous star identification algorithm."1st International Symposium on Systems and Control in Aerospace and Astronautics, Harbin, China, January, 2006, 896-901. DOI:10.1109/ISSCAA.2006.1627471

[9] Benjamin B. Spratling, Iv, and Daniele Mortari. "A survey on star identification algorithms." Algorithms, 2(2009), 93-107.DOI:10.3390/a2010093

[10] Craig L. Cole and John L. Crassidis. "Fast star-pattern recognition using planar triangles." Journal of Guidance, Control, and Dynamics, 29, 1(2006), 64-71. DOI: 10.2514/1.13314

[11] Mortar D., Junkins J. L., and Samaan M. A."Lost-in-space pyramid algorithm for robust star pattern recognition." In 2001 AAS Guidance and Control Conference, Breckenridge, CO, Feb., 2001, 10-12. DOI: 10.1002/j.2161-4296

[12] Mortari, D., Samaan, M. A., Bruccoleri, C., and Junkins, J. L. "The pyramid star identification technique." Navigation.51, 3(2004), 171-183.DOI/10.1002/j.2161-4296

[13] Michael Kolomenkin, Sharon Pollak, IlanShimshoni and Michael Lindenbaum. "Geometric voting algorithm for star trackers." IEEE Transactions on Aerospace and Electronic Systems, 44, 2(2008), 441-456. DOI: 10.1109/TAES.2008.4560198

[14] XieJunfeng, Jiang Wanshou and Gong Jianya. "A new star identification algorithm based on matching probability."In 2008 IEEE International Geoscience and Remote Sensing Symposium - Proceedings, Boston, MA, United states, 2008, 1166-1169. DOI: 10.3390/s150716412

[15] Curtis Padgett and Kenneth Kreutz. "A grid algorithm for autonomous star identification" IEEE Transactions on Aerospace and Electronic Systems, 33, 1(1997), 202-213.DOI: 10.1109/7.570743

[16] Hyunjae Lee and Hyochoong bang. "Star pattern identification technique by modified grid algorithm" IEEE Transactions on Aerospace and Electronic Systems, 43, 3(2007), 1112-1116. DOI: 10.1109/TAES.2007.4383600

[17] Meng Na, Danian Zheng and PeifaJia. "Modified grid algorithm for Noisy all-sky autonomous star identification" IEEE Transactions on Aerospace and Electronic Systems, 45, 2(2009), 516-522. DOI: 10.1109/TAES.2009.5089538

[18] E. Silani and M. Lovera, "Star identification algorithms: Novel approach710 & comparison study," IEEE Trans. Aerosp. Electron. Syst., vol. 42, no. 4,711 pp. 1275–1288, Oct. 2006.

[19] Wei Xingguo, Zhang Guangjun and Jiang Jie. "Full-sky autonomous star identification algorithm based on radial and cyclic feature"In 5th International Symposium on Instrumentation and Control Technology, Beijing, China, 2003, 237-240.DOI. 10.1117/12.521667.

[20] E. Silani, M. Lovera, "Star identification algorithm: Novel approach & comparison study." IEEE Transactions on Aerospace and Electronic Systems, 42, 4(2006), 1275-1288. DOI:10.1109/TAES.2006.314572

[21] Ji Feilong, Jiang Jie,Yan Jinyun. "A Redundant-coded Radial and Neighboring Star Pattern Identification."IEEE Transactions on Aerospace and Electronic Systems. 2015DOI: 10.1109/TAES.2015.140311

[22] LeCun, Y., Bengio, Y. & Hinton, G. Deep learning. Nature 521, 436–444 (2015)DOI :10.1038/nature14539

[23] LeCun, Y., Bottou, L., Bengio, Y. &Haffner, P. "Gradient-based learning applied to document recognition."Proc. IEEE 86, 2278–2324 (1998). DOI: 10.1109/5.726791

[24] He K, Zhang X, Ren S, et al. Deep residual learning for image recognition[C]//Proceedings of the IEEE conference on computer vision and pattern recognition. 2016: 770-778.DOI :10.1109/CVPR.2016.90

[25] Chen L C, Papandreou G, Kokkinos I, et al. Deeplab: Semantic image segmentation with deep convolutional nets, atrous convolution, and fully connected crfs[J]. IEEE transactions on pattern analysis and machine intelligence, 2018, 40(4): 834-848.DOI :10.1109/TPAMI.2017.2699184

[26] He K, Gkioxari G, Dollár P, et al. Mask r-cnn[C]//Computer Vision (ICCV), 2017 IEEE International Conference on. IEEE, 2017: 2980-2988.DOI :10.1109/ICCV.2017.322

Lei Liu is currently a PhD student in the School of Instrumentation Science and Opto-electronics Engineering, BeihangUniversity (BUAA), China.He received her Bachelors, MastersDegreesfromUniversity of Science and Technology Beijing (USTB) from 2006 to 2014.His research interests are image processing and pattern recognition.

Jie Jiang is currently a Professor of the School of Instrumentation Science and Opto-electronics Engineering, Beihang University (BUAA), China. She received her Bachelors, Masters, and Ph.D. degrees from Tianjing University from 1991 to 2000. Her research interests include image processing and star sensors.

GuangjunZhang is currently a Professor in Southeast University, China.He received her Bachelors, Masters, and Ph.D. degrees from Tianjing University from 1982 to 1991. His research interests include image processing and precision measurement.